SUPPORTING INFORMATION

"Strong Electronic Couplings between Ferrocenyl Centers Mediated by Bis-Ethynyl/Butadiynyl Diruthenium Bridges"

Xu, G.-L. *et al.*

Complete References **5** and **91**

5. Adams, D. M.; Brus, L.; Chidsey, C. E. D.; Creager, S.; Creutz, C.; Kagan, C. R.; Kamat, P. V.; Lieberman, M.; Lindsay, S.; Marcus, R. A.; Metzger, R. M.; Michel-Beyerle, M. E.; Miller, J. R.; Newton, M. D.; Rolison, D. R.; Sankey, O.; Schanze, K. S.; Yardley, J.; Zhu, X. Y. *J. Phys. Chem. B* **2003**, *107*, 6668.

91. Frisch, M. J.; Trucks, G. W.; Schlegel, H. B.; Scuseria, G. E.; Robb, M. A.; Cheeseman, J. R.; Montgomery, J. A.; Vreven, T.; Kudin, K. N.; Burant, J. C.; Millam, J. M.; Iyengar, S. S.; Tomasi, J.; Barone, V.; Mennucci, B.; Cossi, M.; Scalmani, G.; Rega, N.; Petersson, G. A.; Nakatsuji, H.; Hada, M.; Ehara, M.; Toyota, K.; Fukuda, R.; Hasegawa, J.; Ishida, M.; Nakajima, T.; Honda, Y.; Kitao, O.; Nakai, H.; Klene, M.; Li, X.; Knox, J. E.; Hratchian, H. P.; Cross, J. B.; Adamo, C.; Jaramillo, J.; Gomperts, R.; Stratmann, R. E.; Yazyev, O.; Austin, A. J.; Cammi, R.; Pomelli, C.; Ochterski, J. W.; Ayala, P. Y.; Morokuma, K.; Voth, G. A.; Salvador, P.; Dannenberg, J. J.; Zakrzewski, V. G.; Dapprich, S.; Daniels, A. D.; Strain, M. C.; Farkas, O.; Malick, D. K.; Rabuck, A. D.; Raghavachari, K.; Foresman, J. B.; Ortiz, J. V.; Cui, Q.; Baboul, A. G.; Clifford, S.; Cioslowski, J.; Stefanov, B. B.; Liu, G.; Liashenko, A.; Piskorz, P.; Komaromi, I.; Martin, R. L.; Fox, D. J.; Keith, T.; Al-Laham, M. A.; Peng, C. Y.; Nanayakkara, A.; Challacombe, M.; Gill, P. M. W.; Johnson, B.; Chen, W.; Wong, M. W.; Gonzalez, C.; Pople, J. A., *Gaussian 03, Revision B.03* (2003) Gaussian, Inc.

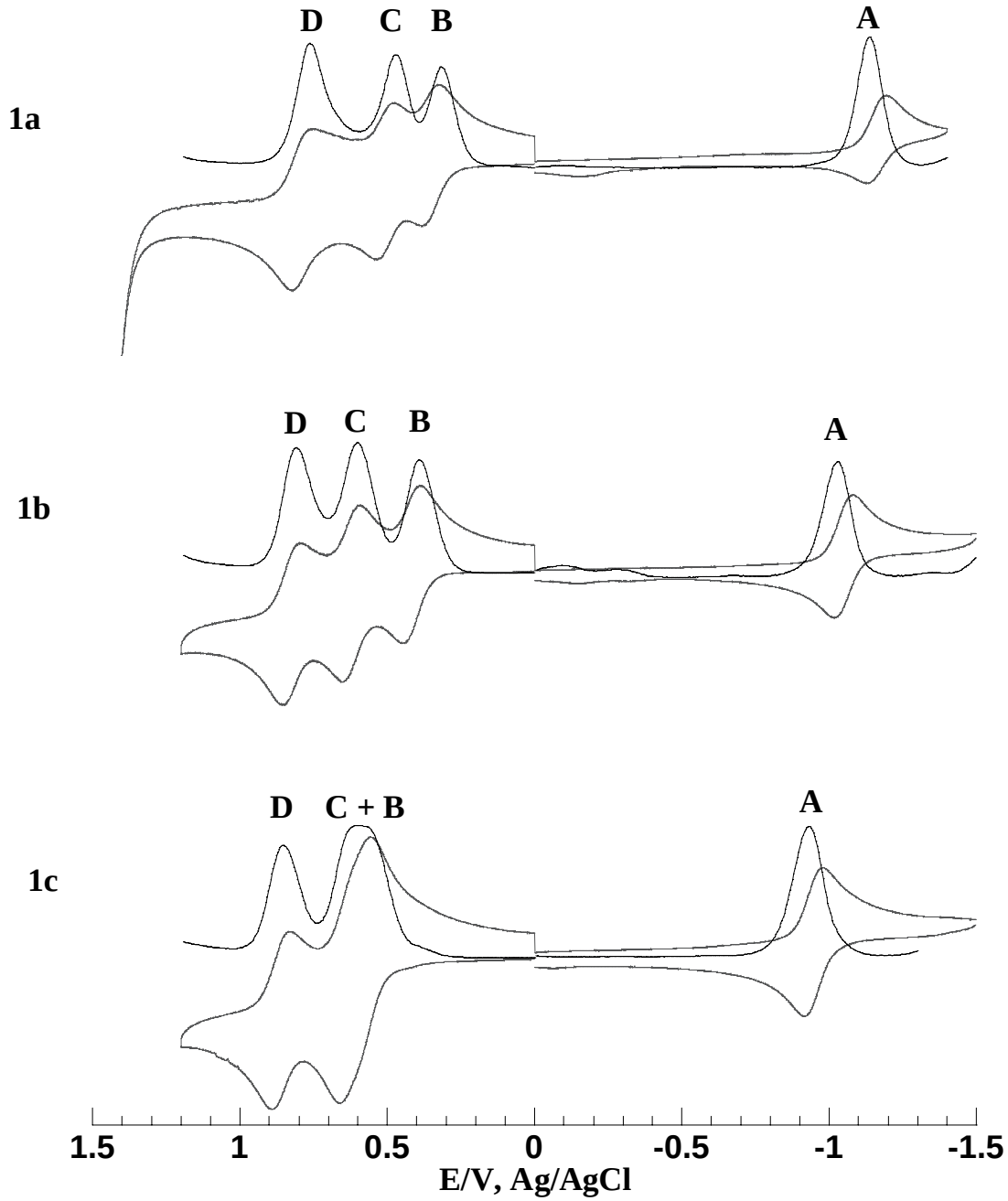

Figure S1. Differential pulse voltammograms (DPV, solid lines) and cyclic voltammograms (CV, thin gray lines) of compounds **1a** – **1c** recorded in 0.20 M THF solution of Bu_4NPF_6.

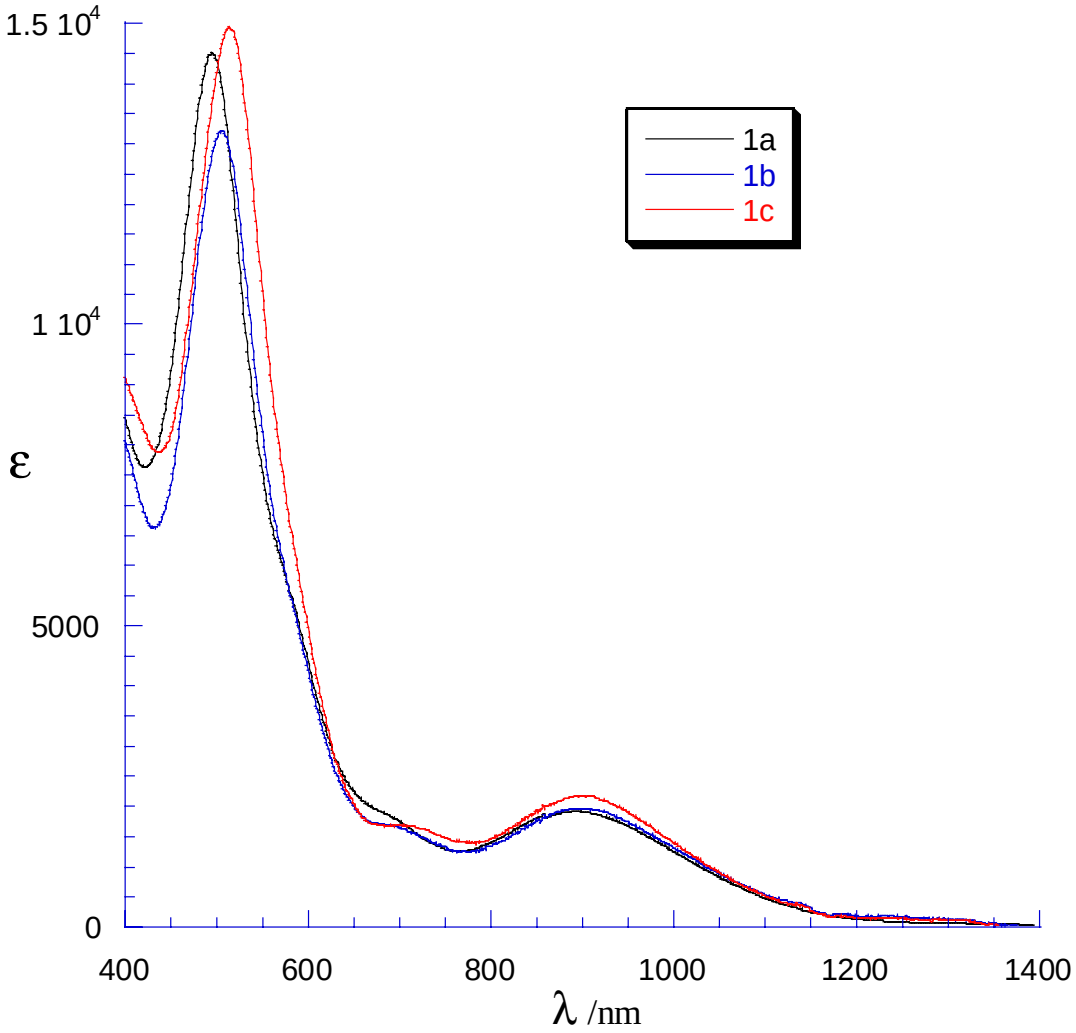

Figure S2. Vis-NIR absorption spectra of compounds **1a** – **1c** recorded in THF.

Preparation of FcC_4SiMe_3. A three-neck flask equipped with an additional funnel was charged with 100 mL of THF, FcC_2H (1.0 g, 4.8 mmol), CuCl (0.200 g) and TMEDA (1 mL). Trimethylsilylacetylene (48.0 mmol (6.8 mL) in 40 mL of THF) was slowly added to the reaction mixture, while air was gently bubbled through the solution. The reaction completed in 6 h as indicated by the disappearance of FcC_2H on TLC. The residue after the solvent removal was purified with silica chromatography to afford FcC_4SiMe_3 as an orange solid (0.560 g, 38% based on FcC_2H). The sample was authenticated by GC-MS.

Computational Details

The model complex, $Ru_2(NHCHNH)_4(C{\equiv}C)_2Fc_2$ (**1**), was employed in the calculations to replace the real complexes, $Ru_2(NRCRNR)_4(C{\equiv}C)_2Fc_2$ (R=CH_3, Ph etc.). By analyzing the structure of $Ru_2(NPhCPhNPh)_4(C{\equiv}C)_2Fc_2$ from the X-ray diffraction, the phenyl ring and NCN ligand are almost perpendicular to each other, indicating no existence of conjugated effect between them. So we use hydrogen atom in place of phenyl group in this work to save the computational resources.

The structure of **1** in the ground state was fully optimized using the density functional method, B3LYP (Becke's 3 parameter hybrid functional using the Lee-Yang-Parr correlation functional). **[1]** Based on the optimized structure, TD-DFT (time-dependent density functional theory) method [**2–4]** was performed to calculate excited states related to absorption spectra of **1**. In these calculations, **1** takes the C_i symmetry according to the X-ray diffraction of $Ru_2(NRCRNR)_4(C{\equiv}C)_2Fc_2$ (R=CH_3 and Ph). **[5]**

In the calculations, quasi-relativistic pseudopotentials of the Ru and Fe atoms proposed by Hay and Wadt **[6]** with 16 and 16 valence electrons, respectively, are employed and the LanL2DZ basis sets associated with the pseudopotential are adopted. All the calculations are accomplished by using the *Gaussian03* program package **[7]**.

Results and Discussion

According to the vertical electron transition mechanism in the absorption process, the optimized ground state geometry was kept, while the TD-DFT (B3LYP) was performed to calculate excited

states related to absorptions. With respect to the ^1A_g ground state under the C_i point group, the $^1A_g \rightarrow {}^1A_u$ transitions are dipole-allowed.

Tables 2 summarized the calculated low-lying absorptions and corresponding oscillator strengths for **1** in the gas phase, respectively, together with experimental data of $Ru_2(NRCRNR)_4(C{\equiv}C)_2Fc_2$ (R=CH_3 and Ph) in the solution. **[5]** To assign the absorptions, the partial molecular orbital contributions (%) involved in the absorption transitions of **1** under the TD-DFT calculations were listed in Tables 3. The coordinate orientation of **1** was depicted in Figure 1, in which the z axis goes through the two Ru atoms.

Under the TD-DFT calculations, the B^1A_u excited state gives rise to about 840 nm absorption, mainly contributed by the $77a_g \rightarrow 80a_u$ configuration with the CI coefficient of 0.58953. According to Table 2, we assigned the absorption to $\pi^*[d_{yz}(Ru_2)]+\sigma[d_z^2(Ru_2)]+\pi[p_y(C{\equiv}C)] \rightarrow \pi^*[d_{xy}(Ru){-}N]+\delta^*[d_{xy}(Ru_2)]$ transition, comparable to the experimental 894 nm absorption. In Figure 3, the electron density diagrams of frontier molecular orbitals related to the 840 nm transitions were depicted, which supports our above assignment. It can be seen that there is a large difference of absorption wavelengths between calculation and experiment. This is just because we only calculate the absorptions of **1** in the gas phase. According to the previous studies **[8]**, the introduction of the solvent effect may results in a large redshift of absorption wavelength.

In addition, we related the calculated 409 nm absorption to experimental 495 nm. Because the absorption has the largest oscillator strength of 0.1895, we think this is most like to be observed

in the experiment. In addition, we displayed the electron density diagrams of frontier orbitals involved in the 409 nm absorption, to intuitively understand the transition process.

1. [a] J. A. Pople, P. M. W. Gill and B. G. Johnson, *Chem. Phys. Lett.* **1992,** 199, 557–560 [b] B. G. Johnson and M. J. Frisch, *J. Chem. Phys.* **1994**, 100, 7429–7442 [c] B. G. Johnson and M. J. Frisch, *Chem. Phys. Lett.* **1993**, 216, 133–140 [d] R. E. Stratmann, J. C. Burant, G. E. Scuseria and M. J. Frisch, *J. Chem. Phys*. **1997**, 106, 10175–10183
2. R. Bauernschmitt, R. Ahlrichs, Chem. Phys. Letters, **1996**, 256, 454–464.
3. N. N. Matsuzawa, A. Ishitani, D. A. Dixon, T. Uda, J. Phys. Chem. A. **2001**, 105, 4953–4962.
4. B. G. Johnson and M. J. Frisch, *J. Chem. Phys.* **1994**, 100, 7429–7442.
5. a) W. R. Wadt, P. J. Hay, *J. Chem. Phys.* **1985,** 82, 284–298; b) P. J. Hay, W. R. Wadt, *J. Chem. Phys.* **1985,** 82, 299–310.
6. G. –L. Xu, M. C. DeRosa, R. J. Crutchley, T. Ren, *J. Am. Chem. Soc.* **2004**, 126, 3728–3729.
7. M. J. Frisch, G. W. Trucks, H. B. Schlegel, G. E. Scuseria, M. A. Robb, J. R. Cheeseman, J. A. Montgomery, Jr., T. Vreven, K. N. Kudin, J. C. Burant, J. M. Millam, S. S. Iyengar, J. Tomasi, V. Barone, B. Mennucci, M. Cossi, G. Scalmani, N. Rega, G. A. Petersson, H. Nakatsuji, M. Hada, M. Ehara, K. Toyota, R. Fukuda, J. Hasegawa, M. Ishida, T. Nakajima, Y. Honda, O. Kitao, H. Nakai, M. Klene, X. Li, J. E. Knox, H. P. Hratchian, J. B. Cross, C. Adamo, J. Jaramillo, R. Gomperts, R. E. Stratmann, O. Yazyev, A. J. Austin, R. Cammi, C. Pomelli, J. W. Ochterski, P. Y. Ayala, K. Morokuma, G. A. Voth, P. Salvador, J. J. Dannenberg, V. G. Zakrzewski, S. Dapprich, A. D. Daniels, M. C. Strain, O. Farkas, D. K. Malick, A. D. Rabuck, K. Raghavachari, J. B. Foresman, J. V. Ortiz, Q. Cui, A. G. Baboul, S. Clifford, J. Cioslowski, B. B. Stefanov, G. Liu, A. Liashenko, P. Piskorz, I. Komaromi, R. L. Martin, D. J. Fox, T. Keith, M. A. Al-Laham, C. Y. Peng, A. Nanayakkara, M. Challacombe, P. M. W. Gill, B. Johnson, W. Chen, M. W. Wong, C. Gonzalez, and J. A. Pople, *Gaussian 03*, *Revision B.03*, Gaussian, Inc., Pittsburgh PA, **2003.**
8. a) Q. –J. Pan, H. –X. Zhang, *Inorg. Chem*. **2004**, 43, 593–601; b) Q. –J. Pan, H. –X. Zhang, *Organometallics* **2004**, 23, 5198-5209; c) Q. –J. Pan, H. –X. Zhang, Eur. J. Inorg. Chem. **2003**, 4202–4210.

Table S1. The optimized main geometry parameters of $Ru_2(Form)_4(C{\equiv}C)_2Fc_2$ at the B3LYP/LanL2DZ level.

Bond length (Å)					Angle (°)				Dihedral angle (°)
Ru–Ru	Ru–N	Ru–C	C≡C	C–C(Cp)	N–Ru–N1	N–Ru–N2	N–Ru–Ru	C–Ru–Ru	N–Ru–Ru–N
2.610	2.031	1.964	1.239	1.428	172.7	89.1	88.8	161.2	179.7

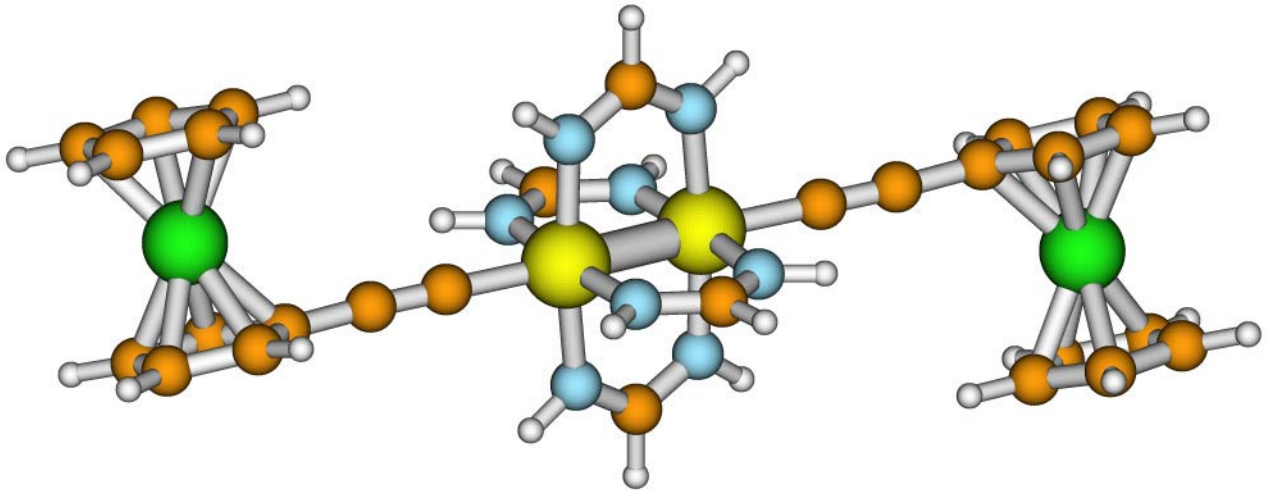

Figure S3. The optimized structure of $Ru_2(Form)_4(C{\equiv}C)_2Fc_2$ at the B3LYP/LanL2DZ level

Table S2. The components of molecular orbitals involved in the transitions for $Ru_2(Form)_4(C{\equiv}C)_2Fc_2$ under the B3LYP/LanL2DZ calculations.

	Energy			Contributions (%)				Components of metal atom(%)	
Orbital	(eV)	Bonding characters	2Ru	4Form	2CC	2Fc	2Fe	Ru	Fe
$91a_u$	0.9755	$\pi^*[p_x(Fe)+\pi(p_x(Ru_2))+ p_x(Fe)]$	6.5	3.0	1.2	89.4	82.0	3.0 p_x	41.0 p
$89a_g$	0.8792	$\sigma^*[sp_z(Ru_2)]+\sigma^*[p_z(C{\equiv}C)]$	44.1	7.3	22.1	26.5	9.0	11.8 s 8.3 p_z	
$88a_g$	0.8019	π^*(Form)	1.8	96.8	0.4	0.9	0.7		
$90a_u$	0.7249	$\pi^*[p_y(Fe)+\pi(p_y(Ru_2))+ p_y(Fe)]$	25.7	12.6	2.1	59.7	44.6	11.1 p_y	22.0 p
$87a_g$	0.7241	$\pi^*[d_{xy}(Ru)–p(N)]+\pi^*(Form)+\delta[d_{xy}(Ru_2)]$	12.2	85.1	1.0	1.7	1.0	4.8 d_{xy}	
$86a_g$	0.6033	$\pi^*[p_xp_y(Ru_2)]+p_x(Fe)$	40.4	5.7	1.2	52.6	43.0	14.5 p_x 5.3 p_y	21.1 p
$89a_u$	0.5538	$p_z(Fe)+ \sigma^*[sp_z(Ru_2)]$	28.3	1.8	11.6	58.3	46.0	6.8 s 5.4 p_z	21.5 p
$85a_g$	0.4596	$p_y(Fe)$	13.5	4.2	0.8	81.4	60.9	3.8 p_y	30.5 p
$88a_u$	0.4430	$\sigma^*[sp_zd_{x^2-y^2}(Ru)–N]+\delta^*[d_{x^2-y^2}(Ru_2)]$	56.6	33.6	2.0	7.7	5.6	13.2 s 6.7 p_z 6.7 $d_{x^2-y^2}$	
$87a_u$	0.3328	$\sigma^*[sp_z(Ru_2)]+ \pi[p_xp_y(Ru_2)]+ \pi^*$(Form)	65.2	15.4	3.4	16.0	11.6	17.8 s 3.0 p_x 3.5 p_y 7.3 p_z	
$84a_g$	0.3124	$p_z(Fe)+\pi[p_yp_z(Ru_2)]$	18.9	13.3	16.4	51.3	38.0	5.1 p_y 3.5 p_z	19.0 p
$86a_u$	0.2961	$\sigma^*[sp_xp_y(Ru)–N]$	41.5	36.5	2.0	20.0	14.2	4.5 s 5.5 p_x 7.0 p_y	
$85a_u$	0.1472	$\sigma^*[sp_z(Ru_2)]$	88.8	6.3	2.4	2.5	1.2	30.4 s 13.1 p_z	
$84a_u$	0.1034	$\pi^*(Form)_{yz}+\pi[p_x(Ru_2)]$	29.4	54.8	1.6	14.3	8.4	7.0 s 4.9 p_x	
$83a_u$	0.0795	$\sigma^*[sp_z(Ru_2)]+\pi^*(Form)_{xz}$	48.7	42.1	5.2	4.0	1.7	16.1 s 4.6 p_z	
$83a_g$	-0.2955	$(d_{xy}+d_{x^2-y^2})(Fe)$	1.3	0.1	0.1	98.4	55.6		7.3 $d_{x^2-y^2}$ 18.0 d_{xy}
$82a_u$	-0.2977	$(d_{xy}+d_{x^2-y^2})(Fe)$	2.4	0.9	0.3	96.4	54.4		7.1 $d_{x^2-y^2}$ 17.5 d_{xy}
$82a_g$	-0.4022	$d_{xz}(Fe)$	3.0	0.9	4.0	92.1	53.3		20.4 d_{xz}
$81a_u$	-0.4346	$d_{xz}(Fe)$	6.9	4.3	5.7	83.1	48.7		17.9 d_{xz}
$81a_g$	-2.1130	$\sigma[(p_z+d_{z^2}+d_{yz})(Ru_2)]+L(C)$	46.8	14.9	35.3	3.1	0.4	4.2 p_z 6.6 d_{z^2} 9.7 d_{yz}	
$80a_u$	-2.9307	$\pi^*[d_{xy}(Ru)–N]+\delta^*[d_{xy}(Ru_2)]$	63.7	35.8	0.3	0.2	0.1	31.4 d_{xy}	
HOMO-LUMO gap									
$80a_g$	-4.7716	$\pi^*[d_{xz}(Ru_2)]+\pi[p_x(C{\equiv}C)]+(d_{z^2}+d_{yz})(Fe)$	42.0	2.6	22.7	32.8	19.1	18.3 d_{xz}	5.1 d_{z^2} 3.0 d_{yz}
$79a_u$	-5.0660	$(d_{z^2}+d_{yz})(Fe)+\pi[p_x(C{\equiv}C)]+\pi[d_{xz}(Ru_2)]$	9.5	3.7	19.0	67.8	51.5	4.3 d_{xz}	14.6 d_{z^2} 7.4 d_{yz}
$78a_u$	-5.2410	$(d_{yz}+d_{z^2})(Fe)$	3.2	0.8	3.8	92.2	78.2		8.3 d_{z^2} 26.1 d_{yz}
$79a_g$	-5.2442	$(d_{yz}+d_{z^2})(Fe)$	3.1	0.3	3.5	93.1	79.1		9.7 d_{z^2} 24.9 d_{yz}
$78a_g$	-5.3533	$d(Fe)+\pi^*[d_{xz}(Ru_2)]$	11.0	0.7	2.5	85.8	69.7	4.8 d_{xz}	15.9 d_{z^2} 3.1 d_{xz} 9.1 d_{yz} 5.5 $d_{x^2-y^2}$
$77a_u$	-5.4957	$d(Fe)+\pi[d_{xz}(Ru_2)]+\pi[p_x(C{\equiv}C)]$	10.9	4.9	16.4	67.8	40.3	5.1 d_{xz}	8.2 d_{z^2} 3.1 d_{xz} 3.0 d_{yz} 4.4 $d_{x^2-y^2}$
$77a_g$	-5.6641	$\pi^*[d_{yz}(Ru_2)]+\sigma[d_{z^2}(Ru_2)]+\pi[p_y(C{\equiv}C)]$	50.8	5.3	30.8	13.1	6.0	8.8 d_{z^2} 12.8 d_{yz}	

$76a_u$	-5.6704	$\pi[d_{yz}(Ru_2)]+\pi[p_y(C\equiv C)]$	42.4	9.2	32.9	15.5	6.8	3.4 d_{z^2} 14.3 d_{yz}	
$76a_g$	-5.7596	$\delta[d_{xy}(Ru_2)]$	71.1	22.2	3.3	3.4	1.0	32.7 d_{xy}	
$75a_u$	-5.8059	$\pi(N)$	0.4	97.0	0.9	1.7	0.4		
$75a_g$	-6.3983	$\pi^*[d_{xz}(Ru_2)]+\delta[d_{xy}(Ru_2)]+\pi(N)$	26.6	39.4	6.0	28.0	3.9	7.7 d_{xz} 3.7 d_{xy}	
$74a_u$	-6.4353	$(d_{x^2-y^2}+d_{z^2}+d_{xy})(Fe)$	0.3	0.0	2.6	97.1	88.5		10.4 d_{z^2} 22.3 $d_{x^2-y^2}$ 10.1 d_{xy}
$74a_g$	-6.4361	$(d_{x^2-y^2}+d_{z^2}+d_{xy})(Fe)$	0.5	0.3	3.0	96.2	86.5		10.2 d_{z^2} 21.8 $d_{x^2-y^2}$ 9.8 d_{xy}
$73a_g$	-6.4706	$\pi(N)_{xz}$	6.5	89.4	1.8	2.3	0.2		
$72a_g$	-6.5422	$\pi(Cp)+\pi(N)_{yz}$	3.8	17.5	0.7	78.0	5.7		
$73a_u$	-6.5428	$\pi(Cp)$	0.1	0.0	0.0	99.8	7.3		
$71a_g$	-6.5441	$\pi^*[d_{xz}(Ru_2)]+\pi(N)_{yz}+\sigma(Fe–Cp)$	10.1	45.3	1.9	42.6	3.3	4.2 d_{xz}	
$72a_u$	-6.8048	$\pi[d_{xz}(Ru_2)]+\sigma(Fe–Cp)$	13.5	4.5	2.6	79.4	13.2	5.9 d_{xz}	3.8 d_{xz}
$70a_g$	-6.9667	$\sigma(Fe–Cp)$	6.5	1.8	5.2	86.4	24.5		9.8 d_{xz}
$69a_g$	-7.0731	$\sigma(Cp–Fe–Cp)$	2.1	0.4	0.8	96.7	28.6		3.7 $d_{x^2-y^2}$ 9.3 d_{xy}
$71a_u$	-7.0764	$\sigma(Cp–Fe–Cp)$	1.2	0.3	0.3	98.2	29.1		3.9 $d_{x^2-y^2}$ 9.4 d_{xy}
$70a_u$	-7.1814	$\pi[d_{xz}(Ru_2)]+\sigma(Fe–Cp)$	32.3	12.8	3.3	51.6	14.1	14.5 d_{xz}	5.4 d_{xz}
$68a_g$	-7.3896	$\pi[d_{yz}(Ru)+p_y(C\equiv C)]+\pi^*[d_{yz}(Ru_2)]$	42.0	9.3	39.6	9.2	1.2	4.6 d_{z^2} 13.6 d_{yz}	
$69a_u$	-7.5142	$\pi[d_{yz}(Ru)+p_y(C\equiv C)]+\pi[d_{yz}(Ru_2)]$	42.7	14.3	36.0	7.0	0.6	4.3 d_{z^2} 13.9 d_{yz}	
$67a_g$	-7.9602	$\pi[p_x(C\equiv C–Cp)]+\pi^*[d_{xz}(Ru_2)]$	7.1	2.8	37.8	52.3	10.1	3.0 d_{xz}	
$68a_u$	-8.0579	$\pi[p_x(C\equiv C–Cp)]+\pi(N)_{xz}$	9.3	32.2	27.1	31.5	6.5		
$67a_u$	-8.1436	$\sigma(Ru–N)_{yz}$	11.6	85.6	2.3	0.5	0.1		
$66a_u$	-8.2114	$\sigma(Ru–N)_{xz}$	24.6	67.6	4.3	3.5	0.6	8.4 d_{xz}	
$65a_u$	-8.8462	$\pi[d_{xy}(Ru)–p(N)$	38.3	58.8	1.8	1.0	0.2	18.8 d_{xy}	

Table S3. Calculated absorptions of $Ru_2(Form)_4(C{\equiv}C)_2Fc_2$ in the gas phase at the TD-DFT (B3LYP) level.

			Transition Energy			
States	Configuration	|CI Coef.| > 0.2	eV	nm	f^a	Exp.
^1A_u	$80a_g \rightarrow 80a_u$	0.61161	0.76	1642	0.0007	
^1A_u	$77a_g \rightarrow 80a_u$	0.58953	1.48	840	0.0002	894 (1194)
	$79a_g \rightarrow 80a_u$	0.29788				
^1A_u	$78a_g \rightarrow 81a_u$	–0.32538	1.75	708	0.0056	
	$79a_g \rightarrow 82a_u$	0.33630				
	$78a_u \rightarrow 83a_g$	0.33862				
	$79a_u \rightarrow 82a_g$	–0.30601				
	$77a_u \rightarrow 82a_g$	–0.23210				
^1A_u	$78a_g \rightarrow 80a_u$	0.65319	1.95	637	0.0012	
	$80a_g \rightarrow 80a_u$	–0.20678				
^1A_u	$79a_g \rightarrow 80a_u$	0.63588	1.97	630	0.0003	
	$77a_g \rightarrow 80a_u$	–0.28852				
^1A_u	$79a_u \rightarrow 81a_g$	0.56949	2.14	578	0.0009	
	$77a_u \rightarrow 81a_g$	–0.27356				
^1A_u	$76a_u \rightarrow 81a_g$	–0.44361	2.18	570	0.0024	
	$76a_g \rightarrow 80a_u$	0.40672				
	$78a_u \rightarrow 81a_g$	–0.21183				
^1A_u	$74a_g \rightarrow 81a_u$	–0.30551	2.27	546	0.0047	
	$74a_u \rightarrow 82a_g$	–0.31271				
	$79a_g \rightarrow 82a_u$	0.26585				
	$78a_u \rightarrow 83a_g$	0.26615				
^1A_u	$75a_g \rightarrow 80a_u$	0.44245	2.59	479	0.0702	
	$76a_g \rightarrow 80a_u$	0.26617				
	$78a_u \rightarrow 81a_g$	0.25366				
^1A_u	$75a_u \rightarrow 81a_g$	0.65652	2.66	465	0.0003	
^1A_u	$78a_u \rightarrow 81a_g$	0.60602	2.75	451	0.0058	
	$75a_g \rightarrow 80a_u$	–0.22285				
	$76a_u \rightarrow 81a_g$	–0.21544				
^1A_u	$77a_u \rightarrow 81a_g$	0.58354	2.83	437	0.0010	
	$79a_u \rightarrow 81a_g$	0.29348				
	$75a_u \rightarrow 81a_g$	0.23171				
^1A_u	$73a_g \rightarrow 80a_u$	0.45478	2.89	429	0.0630	
	$71a_g \rightarrow 80a_u$	–0.25363				
	$76a_u \rightarrow 81a_g$	0.21639				
	$75a_g \rightarrow 80a_u$	–0.20783				
^1A_u	$71a_g \rightarrow 80a_u$	0.45848	2.94	422	0.0551	
	$72a_g \rightarrow 80a_u$	–0.29077				
	$73a_g \rightarrow 80a_u$	0.24945				
	$75a_g \rightarrow 80a_u$	–0.24249				

^1A_u	$73a_g \rightarrow 80a_u$	0.35492	3.03	409	0.1895	495 (9068)
	$75a_g \rightarrow 80a_u$	0.26346				
	$76a_g \rightarrow 80a_u$	–0.24247				
	$76a_u \rightarrow 81a_g$	–0.29331				
^1A_u	$74a_g \rightarrow 81a_u$	0.36037	3.22	385	0.0002	
	$74a_u \rightarrow 82a_g$	0.36710				
^1A_u	$71a_g \rightarrow 80a_u$	0.36459	3.23	384	0.0005	
	$72a_g \rightarrow 80a_u$	0.59930				
^1A_u	$68a_g \rightarrow 80a_u$	0.62284	3.43	362	0.0076	
	$69a_g \rightarrow 80a_u$	0.22278				
^1A_u	$70a_g \rightarrow 80a_u$	0.67996	3.60	344	0.0006	
^1A_u	$70a_u \rightarrow 81a_g$	0.33425	3.79	327	0.0003	
	$72a_u \rightarrow 81a_g$	0.33386				
	$69a_g \rightarrow 80a_u$	0.27885				
^1A_u	$80a_g \rightarrow 82a_u$	0.51363	3.89	319	0.0045	
	$77a_u \rightarrow 83a_g$	0.29860				
	$78a_g \rightarrow 82a_u$	0.26584				
^1A_u	$80a_g \rightarrow 81a_u$	0.56539	3.89	319	0.3269	
	$78a_g \rightarrow 81a_u$	0.23520				
^1A_u	$74a_u \rightarrow 81a_g$	0.68096	3.91	317	0.0344	
^1A_u	$80a_g \rightarrow 83a_u$	0.44972	4.02	309	0.0007	
	$80a_g \rightarrow 86a_u$	–0.20837				
	$80a_g \rightarrow 88a_u$	–0.31343				

a. Oscillator strength.